

Long-term trends at the Time Series Station Boknis Eck (Baltic Sea), 1957–2013: does climate change counteract the decline in eutrophication?

S. T. Lennartz¹, A. Lehmann¹, J. Herrford¹, F. Malien¹, H.-P. Hansen¹, H. Biester², and H. W. Bange¹

¹GEOMAR Helmholtz-Centre for Ocean Research Kiel, Düsternbrooker Weg 20, 24105 Kiel, Germany

²TU Braunschweig, AG Umweltgeochemie, Institute of Geoecology, Langer Kamp 19c, 38106 Braunschweig, Germany

Correspondence to: S. T. Lennartz (slennartz@geomar.de)

Abstract

The Time Series Station Boknis Eck (BE), initiated in 1957, is one of the longest operated time series stations worldwide. We present the first statistical evaluation of a dataset of nine physical, chemical and biological parameters in the period of 1957–2013. In the past 3 to 5 decades, all of the measured parameters underwent significant long-term changes. Most striking is an ongoing decline in bottom water oxygen concentration, despite a significant decrease of nutrient and chlorophyll *a* concentrations. Temperature enhanced oxygen consumption in the bottom water and a prolongation of the stratification period are discussed as possible reasons for the ongoing oxygen decline despite declining eutrophication. Observations at the location BE were compared with model output of the Kiel Baltic Sea Ice Ocean Model (BSIOM). Reproduced trends were in good agreement with observed trends for temperature and oxygen, but generally the oxygen concentration at the bottom has been overestimated.

1 Introduction

Long-term observations in oceanography are crucial when it comes to improving the understanding of the state of ecosystems and monitoring their long-term developments. They have been a core strategy in the last 50 decades and are still considered to have high priority today (see e.g. Ducklow et al., 2009), as they enable the quantification of long-term trends, the identification of regime shifts and the characterization of processes that help to predict future development.

Long-term monitoring is especially important for a dynamic system such as the Baltic Sea, where high variations, which are effective on different time scales, are triggered by natural and anthropogenic causes. The natural hydrographic setting of the Baltic Sea is defined by the small connection to the North Sea, where water exchange takes place through the Danish Straits. The Baltic Sea displays a strong stratification throughout the year, resulting from differences in the salinity of different water masses (Rheinheimer and Nehring,

1995). On a shorter time scale, major salt water inflows triggered by westerly winds transport large amounts of full saline North Sea water into the Baltic Sea (Hanninen et al., 2000; Lass and Matthäus, 1996).

Over decadal time scales, anthropogenic influences like eutrophication have been impacting the ecosystem of the Baltic Sea. Marine eutrophication caused by enhanced nutrient input is a widespread phenomenon in coastal areas worldwide, and in the Baltic Sea in particular (HELCOM, 2009). Generally, nutrient concentrations have risen until the mid 1980ies due to excess riverine input of phosphate and nitrate (Babenerd, 1991; Rosenberg, 1990; HELCOM, 2009), with consequences such as severe deoxygenation (Diaz and Rosenberg, 2008; HELCOM, 2009). The trend in eutrophication and severely rising nutrients has been stopped or even reversed (HELCOM, 2009; Carstensen et al., 2006) since the Helsinki Commission (HELCOM) in 1974 was established to reduce anthropogenic caused marine eutrophication in the Baltic Sea (HELCOM, 1974).

Although the Baltic Sea is one of the best studied coastal areas (Feistel et al., 2008; BACC, 2008), time series dating back to the 1950s are sparse. The time series at BE was initiated in 1957 and thus provides continuous information on changes in the southwestern Baltic Sea over more than five decades (Bange et al., 2011). In this study, we present and statistically evaluate a monthly dataset of nine physical, chemical and biological parameters observed over a time span of 56 years at Boknis Eck. One focus is the detailed analysis of decadal variability and climatic changes occurring over the entire time span. Decadal climate variability was analysed by evaluating the variation in physical parameters such as temperature, salinity and the density gradient in the water column as an indicator for stability of stratification. The second focus addressed was eutrophication, including the analysis of nutrient and chlorophyll *a* concentration in the mid water column and oxygen content in the bottom water. In a further step, long-term trends were compared to the model output of the Baltic Sea Ice Ocean Model (BSIOM). This approach aims to combine the advantages of both direct measurements as well as spatially and temporarily highly resolved model output.

2 Data and methods

2.1 Time Series Station Boknis Eck

The Time Series Station Boknis Eck (BE) is located at the entrance of the Eckernförde Bay (54°31' N, 10°02' E, 28 m water depth, Fig. 1) in the southwestern Baltic Sea. The monitoring of a variety of physical, chemical and biological parameters was initiated by Johannes Krey (Institut für Meereskunde, Kiel) in 1957 (Krey et al., 1980), and has been operated since then on a monthly basis with only two major breaks in 1975–1979 and 1983–1985, where no data is available (Fig. 2).

Starting with measurements of temperature, salinity and oxygen on 30 April 1957, the number of parameters has increased almost continuously. Chlorophyll *a* (since 1960) and nutrients like nitrate, ammonium (1979), nitrite (1986) and phosphate (1957–1966, since 1979) are now part of the monthly routine (Fig. 2). Measurement techniques changed only once for temperature, salinity, phosphate and chlorophyll *a* (1), all of which were calibrated so that no shifts in the trends due to a change in measurement techniques is expected. A more detailed summary on the parameters and applied methods can be found in Table 1 and on the Boknis Eck homepage www.bokniseck.de.

The routine of measurements and analysis has changed little during the observation period. Monthly samples have been taken from research vessels during half-day trips, the sampling usually starting around 9 to 10 in the morning. Sea water has been sampled at 6 standard depths (0.5 or 1 m, 5 m, 10 m, 15 m, 20 m, 25 or 26 m) using Niskin Bottles or the like during several casts, prepared on board and cooled until further analysis. Analysis was usually carried out in the days following the cruise.

The time series of BE provides a highly valuable dataset for three main reasons. Firstly, the time span of observation covers 56 years and hence provides continuous information on changes in the time span of decades. Secondly, there have only been minor changes in the methods used for determining the parameters, and careful calibration avoided shifts or inaccuracies in the data. This consistency strongly enhances the quality of the data, as shifts in the data signals through different methods of analysis can be excluded. Thirdly, the

location of Boknis Eck was initially chosen because it reflects the hydrographic setting of the Kiel Bight (Krey et al., 1980). As there are no major rivers discharging into the Eckernförde Bay, riverine inputs of e.g. nutrients can be neglected, however, influences by direct runoff from land cannot be excluded.

2.2 Statistical analysis

The complete time series of nine parameters covering the period from 1957 to 2013 is described and statistically evaluated for the first time. Statistical tests covering the long-term development of median (Mann–Kendall–Test (MKT), Sen’s slope) and extreme values (quantile regression of 10 and 90 percentile) were applied (details see below). Prior to the analysis, data were averaged as sampling was conducted in slightly different standard depths (differences 1 m) or additional depths in the described period. Thus, data were averaged to the following ranges: 0–2.5 m, 3–7.5 m, 8–12.5 m, 13 to 17.5 m, 18 to 22.5 m and > 23 m. The ranges are referred to as 1 m, 5 m, 10 m, 15 m, 20 m and 25 m. For the MKT and for descriptive statistics, the averaged raw data including irregular spacing and missing values were used.

The measurements were averaged in cases of several dates per month (<5 %) and assumed to be representative for the whole month. Therefore, the corresponding date was chosen to be the middle of the month (15th). Gaps were filled by linear interpolation in case of one or two missing months in a row; larger gaps were filled by replacement with the median of the corresponding month. In case of missing values, the temperature at the surface (1 m) was replaced by the model output of the Baltic Sea-Ice Ocean Model (Lehmann et al., 2014).

Beside the measured parameters, oxygen saturation and density gradient were derived from measurements. Density was calculated using the UNESCO algorithm for density in seawater (UNESCO, 1981). Oxygen saturation was calculated according to Eq. 1, with the measured concentration C_m and the equilibrium concentration C_a according to Garcia and

Gordon (1992) using temperature and salinity from the BE time series:

$$\text{Sat}_{\text{oxy}}[\%] = \frac{C_m}{C_a} \times 100 \quad (1)$$

The nutrient concentrations in 10 m depth were treated differently than the physical parameters, due to their different seasonality. As nutrients become limiting during summer (Wasmund et al., 2011), their concentration is very low between March and September and does not show large variations. A general method to decipher trends in nutrients is to consider the means of December, January and February (DJF) for each winter period, which were simply linearly regressed. Phosphate and ammonium were additionally analysed in the bottom layer, using the monthly MKT for each month individually.

2.2.1 Mann–Kendall–Test

The Mann–Kendall–Test (MKT) is a nonparametric, statistical test to decipher significant monotonic long-term trends in time series. The MKT tests the null hypothesis that all variables are randomly distributed against the alternative hypothesis that a monotonic trend exists in the time series on a given significance level α (here $\alpha = 0.05$). The test statistics of the MKT can be found in Hirsch and Slack (1984).

The MKT can be modified to decipher trends in seasonal data, e.g. monthly data like the BE time series, when a homogeneous trend is present (Hirsch and Slack, 1984). A seasonal MKT including all seasons was performed when trends in the individual months were homogeneous, otherwise the months were tested individually.

If a trend is present in the time series according to the MKT, a median slope was computed according to Sen (1968). The MKT test was applied to the raw data including missing and tied values, the latter were averaged within the MKT function. For the test, a MatLab function from Burkey (2012) based on the MKT accounting for serial correlation by Hirsch and Slack (1984) and Sen (1968) was used.

2.2.2 Quantile regression

The de- or increase of extreme values within the time series was evaluated by quantile regression, which is a least-squares optimisation technique to find the conditional quantile in a time series (Koenker and Hallock, 2001).

To assess the significance of the trend, the method proposed by Franzke (2013) was applied, using a constrained Monte-Carlo approach to generate surrogate data. Quantile regression was then applied to each of the surrogate data sets. A statistically significant trend was present if the trend in the original time series lay outside of the 95% boundaries of the trends for the surrogate data, which equals a level of significance $\alpha=0.1$ (two-sided). The surrogate data were generated by following an approach of Schreiber and Schmitz (1996). They proposed an iterative algorithm that generates time series with the same power spectrum and the same range of values. Details can be found in their paper, and are only briefly summarized here: surrogate data were generated by (i) Fourier transforming and randomly shuffling of the original time series, (ii) replacing the amplitudes of the old time series by the new one and Fourier transforming it inversely afterwards, (iii) rank ordering of the new time series according to the value spectrum of the old time series, (iiii) repeating steps (ii) and (iii) until convergence.

Following this approach, 500 surrogate time series were generated. As the generation of the surrogate data required complete time series, both the quantile regression and the generation of the data sets were performed with the interpolated and gap-filled time series.

2.3 Hydrodynamic model of the Baltic Sea

The numerical model used in this study is a three-dimensional coupled sea-ice ocean model of the Baltic Sea (BSIOM, Lehmann and Hinrichsen, 2000; Lehmann et al., 2002). The horizontal resolution of the coupled sea-ice ocean model is at present 2.5 km, and 60 levels are specified in the vertical, which enables the upper 100 m to be resolved into levels of 3 m thickness. The model domain comprises the Baltic Sea, including the Kattegat and the Skagerrak. At the western boundary, a simplified North Sea basin is connected to the

Skagerrak to supply characteristic North Sea water masses in terms of temperature and salinity profiles resulting from the different forcing conditions (Lehmann, 1995). Prescribed low frequency sea level variations in the North Sea/Skagerrak were calculated from the BSI (Baltic Sea Index, Lehmann et al., 2002; Novotny et al., 2006). The coupled sea-ice ocean model is forced by realistic atmospheric conditions taken from the Swedish Meteorological and Hydrological Institute (SMHI Norrköping, Sweden) meteorological database (L. Meuller, personal communication) which covers the whole Baltic drainage basin on a regular grid of $1^\circ \times 1^\circ$ with a temporal increment of 3 h. The database consists of synoptic measurements that were interpolated on the regular grid with a two-dimensional optimum interpolation scheme. This database, which for modelling purposes was further interpolated onto the model grid, includes surface pressure, precipitation, cloudiness, air temperature and water vapour mixing ratio at 2 m height and geostrophic wind. Wind speed and direction at 10 m height were calculated from geostrophic winds with respect to different degrees of roughness on the open sea and off the coast (Bumke et al., 1998). BSIOM forcing functions, such as wind stress, radiation and heat fluxes were calculated according to Rudolph and Lehmann (2006). Additionally, river runoff was prescribed from a monthly mean runoff data set (Kronsell and Andersson, 2012). The numerical model BSIOM has been run for the period 1970–2010.

The oxygen consumption sub-model (OXYCON: Hansen and Bendtsen, 2009; Jonasson et al., 2012) describes one pelagic oxygen sink and two benthic sinks due to microbial and macrofaunal respiration. Pelagic and benthic oxygen consumption is modelled as a function of temperature and oxygen concentration. Originally, Hansen and Bendtsen (2009) developed OXYCON for the North Sea–Baltic Sea transition area including the Kattegat and the Belt Sea. They estimated an annual average of primary production to be 160 g C m^{-2} for this area (Bendtsen and Hansen, 2013). However, a constant rate of primary production is not suitable when simulating the entire Baltic Sea. Wasmund et al. (2001) compiled primary production data resolved for the different sub-basins of the Baltic Sea, covering two time periods around 1970–1980 and 1990–2000, respectively. Over the period of about 20 years, primary production nearly doubled in almost all regions of the Baltic Sea. According to

these changes in primary production, oxygen consumption rates were linearly increased from 1970 until 1997, and kept constant afterwards. At the sea surface, the oxygen flux is based on the oxygen saturation concentration determined from the modelled sea surface temperature and salinity values. The BSIOM-OXYCON model has been extensively validated in Lehmann et al. (2014).

For comparison, mean values of the water column in both measured and modeled parameters were compared. Averaging was necessary as the model had a higher spatial resolution than the sampling. Model output on the location Boknis Eck at the day of sampling was compared to the measurements by linear regression and the deviation from the bisectrix in the regression plot.

Furthermore, linear regression was performed with daily as well as with monthly (day of BE observations) model output to assess the trends in modelled temperature, salinity and oxygen content. These were compared to the linear regression of the monthly observation of these three parameters at Boknis Eck.

To test the hypothesis of altered stratification, the development of the thermocline was further investigated with the model output of the BSIOM. Different criteria in temperature difference across the thermocline were applied and the trend in the length of the stratification period was assessed by linear regression.

3 Results

3.1 Long-term trends in the BE-Time Series

3.1.1 Temperature

Surface temperature was dominated by a clear seasonal cycle (Fig. 4). However, the cycles in different depths were asynchronous, thus a thermal gradient and consequently a stratification in the water column occurred. During the period 1957 to 2013, the months January to March exhibited an almost homogeneously tempered water column. A thermocline usually developed in March/April and lasted until October in a depth of 10 to 15 m (Fig. 3).

Temperature significantly increased in January, April and May, with rising trends between $0.03\text{--}0.06\text{ }^{\circ}\text{C yr}^{-1}$ (Table 2). The overall increase was $0.018\text{ }^{\circ}\text{C yr}^{-1}$, but was not significant. Testing for trends in the extreme values, e.g. the 10 and 90 % quantile, yielded positive tendencies for both quantiles, but they were not significant ($p > 0.05$, Table 4). Tendencies in extreme values and mean were similar.

The temperature distributions for August, usually the warmest month in a year, revealed that during the second half of the series from 1985 onwards, warmer temperature anomalies increased in frequency (Fig. 6). Anomalies of up to $+2.2\text{ }^{\circ}\text{C}$ (1997, 2003) occurred, while the mean did not shift significantly.

The temperature in 25 m showed a similar strong annual cycle as the surface, but the warming pattern was different. Highest temperatures usually occurred in October, lowest during February. Warming tendencies could be detected for all months, with significant warming in the period January to April as well as for June and September (Table 2).

3.1.2 Salinity

The bottom water salinity in 25 m depth displayed strong fluctuations (Fig. 4), but did not have a regular annual cycle. The mean salinity was 26.6 ± 2.0 and varied in a mean range of 2.9. The high bottom salinity indicates an origin from the Kattegat surface water, which enters the Danish Straits as dense bottom current. The bottom water moves to the south, through the Little and Great Belt, entering Kiel Bight from the north and east, finally arriving at Eckernförde Bay. On average, the lowest salinity was present in March and the highest in August and September, but there was variation in the timing of the maxima and minima. A halocline is present throughout the year, with stronger gradients in summer (March–October, Fig. 3).

No significant trend was detectable with the seasonal MKT for salinity in the period from 1957 to 2013 (Table 4), although short term variations were present over a relatively large range (about 22 %). However, salinity increased slightly, but significantly by 0.04 yr^{-1} (March) and 0.06 yr^{-1} (April) (Table 2). Negative tendencies were present in the period between July and October, but these were not significant. All other tendencies were positive

but also not significant. Testing for a trend in extreme values revealed a significant increase in the 10 % quantiles ($+0.025 \text{ yr}^{-1}$) (Table 4). The correlation between oxygen and salinity in the bottom water was not significant at the $\alpha=0.05$ level.

3.1.3 Oxygen

Oxygen concentration in 25 m depth was dominated by an annual cycle with the highest concentration in March and the lowest in September (Fig. 4). They were decreasing with a median slope (Sen's slope) of $-0.9 \mu\text{mol L}^{-1} \text{ yr}^{-1}$ (Table 4). To better resolve the trends for individual months, the MKT was conducted for each month individually. A significant decreasing trend could be detected in January and for the summer months from April to September in a range of $-0.5 \mu\text{mol L}^{-1} \text{ yr}^{-1}$ (July) and $-0.8 \mu\text{mol L}^{-1} \text{ yr}^{-1}$ (April) (Table 2). The concentrations of the 10 % quantile significantly decreased as well, with a similar intensity of $-0.78 \mu\text{mol L}^{-1} \text{ yr}^{-1}$ (Table 4). The number of anoxic and suboxic events (here $< 10 \mu\text{mol L}^{-1} \text{ O}_2$) has increased continuously since the 1970s (Fig. 7).

Similar trends were found in oxygen saturation calculated from measured oxygen concentrations, temperature and salinity (Eq. 1). Monthly MKT for oxygen saturation yielded significant decrease in January, April, May, July and September in a range of $-0.26 \% \text{ yr}^{-1}$ (January) to $-0.47 \% \text{ yr}^{-1}$ (July) (Table 2).

3.1.4 Density gradient

The density gradient varied seasonally with minima during winter and maxima during summer months. Significant trends could be found for three months: the highest significant increase was found in April, when the gradient rose by $0.002 \text{ kg m}^{-4} \text{ yr}^{-1}$. Significant negative but weaker trends were detected in July and October (both $-0.001 \text{ kg m}^{-4} \text{ yr}^{-1}$) (Table 2).

3.1.5 Phosphate

The phosphate concentration in the mid water column (10 m depth) displayed regular seasonal dynamics throughout the whole sequence 1957 to 2013 (despite the major gap in

measurements from 1966–1986). During the winter months December to February, the highest concentrations were present. During the summer months April to July, the mean as well as the variations between years were smaller with $0.12 \pm 0.15 \mu\text{mol L}^{-1}$.

Phosphate was the only series where the standard deviation fluctuated intensively after the gap filling from 1967–1979 and 1983–1986. Hence, for the MKT, only the time series starting on 7 January 1986, is used. Testing for monthly trends revealed significant negative trends for the winter months December to March as well as September (Table 3). The strongest decrease was detected in December, the weakest in September. To compare the nutrients among each other, the concentrations during the winter months December, January and February were averaged and linear regression was performed, which yielded a linear decrease of $-0.095 \mu\text{mol L}^{-1} \text{yr}^{-1}$ for phosphate (Table 5, Fig. 5). Phosphate concentrations in the period after 1986 decreased, but did not yet reach the level of concentrations in the beginning 1960s. (Fig. 5)

The phosphate concentration at 25 m near the sediment varied seasonally, but the seasonal variation differed strongly from the one at 10 m depth. The yearly maximum in 25 m depth was in October, not in January as in the 10 m time series (Fig. 3). Here, the phosphate concentrations were in average $0.95 \pm 0.72 \mu\text{mol L}^{-1}$ throughout the year except for the months September and October. During these months, the concentration was elevated to $3.7 \pm 3.4 \mu\text{mol L}^{-1}$, which is considerably higher than the maxima in 10 m depth. The elevated concentration in these months was coincident with the lowest oxygen concentrations during the course of one year. Negative trends in phosphate concentrations were present in the winter and spring months January to April (Table 3). A decrease of $-0.1 \mu\text{mol L}^{-1}$ per year was present in the September data, which is one order of magnitude higher as the other significant trends (3).

3.1.6 Nitrate

The seasonal dynamic of the nitrate concentration at 10 m was similar to the dynamic of phosphate concentration in the same depth. Nitrate concentrations were highest in the winter months December to February with the maximum in February. Measurements were

only continuously available since 1986, thus the trends refer only to the period 1986–2013. MKT was performed for the months individually as heterogeneous monthly trends were present. Nitrate concentrations decreased significantly between December and April for the period 1986 to 2013. The decrease was strongest in February with a decrease of $-0.3 \mu\text{mol L}^{-1} \text{yr}^{-1}$ (Table 3). For the winter months DJF, linear regression yielded a decrease of $-0.16 \mu\text{mol L}^{-1} \text{yr}^{-1}$ (Fig. 5).

3.1.7 Nitrite

The nitrite concentration in 10 m depth showed a similar seasonality as the nutrients described above (Fig. 3). During the summer months April to September, the concentration was in average in the range of $0.05\text{--}0.01 \mu\text{mol L}^{-1}$ with the highest concentration of that period in June and the lowest in September and October. However, during the winter months in January and February, the concentration was on average the highest during each year.

Nitrite measurements have only been available since 1988, and the trends only refer to this period. No homogeneous trends could be detected for all seasons, hence the months were tested individually for a long-term trend. A significant downward trend was evident in January, March and April (Table 3). The linear regression for the winter months DJF showed a decreasing trend of $-0.0085 \mu\text{mol L}^{-1} \text{yr}^{-1}$ (Fig. 5).

3.1.8 Ammonium

Ammonium concentration in 10 m depth displayed a similar seasonal cycle as the other nutrients in the same depth with higher concentrations during the winter months December to February and lower concentrations during summer (Fig. 3). During the summer months, the concentrations were in a mean range of $0.44 \pm 0.45 \mu\text{mol L}^{-1}$ (October) to $0.87 \pm 1.73 \mu\text{mol L}^{-1}$ (March). For the MKT, only the time series after 1986 were considered, as continuous data before 1986 was sparse. No homogenous trend could be detected for the series including all months, so the months were tested individually. Decreasing trends were present in the months of January to April (Table 3). In August, a significant increasing

trend was detected. If a linear trend is assumed for the year to year variation of the winter months DJF, the decrease is $-0.14 \mu\text{mol L}^{-1} \text{yr}^{-1}$ (Fig. 5).

The ammonium concentration in 25 m depth displayed a different seasonality. In general, the mean concentration was higher as in 10 m. Furthermore, the seasonal cycle had its yearly maxima on average in May and in October, and not during the winter months as in 10 m depth. Trends were again only evaluated for the period after 1986 and were tested individually as well, as there was no homogenous trend for all seasons present. However, none of the trends were significant.

3.1.9 Chlorophyll *a*

The mean yearly distribution of the chlorophyll *a* concentration in the water column displayed clear seasonal variations (Fig. 3). Throughout the water column, the concentrations were highest in March. In opposite to this spring peak, the maximal values for the second maximum in a year were more diversely distributed among the months August to December and hence the second maximum could not be dated to a single month. The time series was segmented in two main parts, ranging from 1960–1975 (I) and 1988–2012 (II). These series differed considerably in mean chlorophyll *a* concentrations and were therefore analysed separately (Fig. 4). During the first series (I), chlorophyll *a* concentrations were on average $5.57 \pm 6.39 \mu\text{g L}^{-1}$. In series II, the average concentration was lower with $2.85 \pm 2.20 \mu\text{g L}^{-1}$. However, the average seasonality did not change, as the highest mean concentrations in both series were detected in March and during a second maximum in fall. The lowest concentrations per year were most often found in January.

The two parts of the time series were separately tested for trends with the MKT. Chlorophyll *a* concentrations in series I did show a homogenous tendency, but no significant trend could be detected (Table 2). For series II, concentrations were rising significantly in February with an increase of $0.06 \mu\text{g L}^{-1}$. Significant negative trends were detected in April, May, July and October (Table 2). In the trends of the extreme values, e.g. the 90 %-quantile, a significant trend was detected for series II. The quantile is decreasing with $-0.12 \mu\text{g L}^{-1} \text{yr}^{-1}$, which is twice as high as the median decrease computed with Sen's slope (Table 4).

3.1.10 Secchi Depth

Secchi Depth displayed fluctuations throughout the whole period from 1986 to 2013 (not shown). The mean Secchi depth was 6.8 ± 1.8 m with a mean amplitude of 2.1 m. The shallowest Secchi depth usually occurs in March (6.1 m), the deepest in January (8.2 m).
5 Although a negative median slope was present, this was not significant ($p = 0.9$). However, extremely deep Secchi depths decreased, indicated by the regression of the 90 % quantile, which decreased 0.08 m per year (Table 2).

3.2 Model accuracy at the BE location

In general, the model output for the location of Boknis Eck was in varying but overall good
10 agreement with the observations in the 1 : 1 comparison, the trend and the averages of the parameters temperature, salinity and oxygen. Observed temperature agreed best with model output, especially at the surface ($R^2 = 0.98$, Fig. 8). The linear trend in the period 1970–2010 was captured very well when only the days with measurements at BE were considered (Table 6), which resulted in a difference of 0.1°C per decade. However, it differed
15 from the trend when all the days were considered by 0.3°C per decade. Also the mean observed and modeled temperature agreed very well in both the surface and bottom layer. In the bottom layer, the trends were identical no matter which temporal resolution was considered for trend calculation. This is not surprising because the temperature evolution is tied to the atmospheric forcing, i.e. boundary conditions. Modelled salinity agreed less accu-
20 rate than temperature with the observations. The salinity evolution is coupled to the overall water budget including the net freshwater flux and western boundary condition for salinity which are much more uncertain. The trends in model and observations showed different directions, but were both non-significant and very small compared to the general salinity of approx. 22 (Table 6). Furthermore, the model overestimated oxygen concentrations in the
25 bottom layer substantially, the surface layer concentrations however were met except for periods where extremely low oxygen conditions prevailed (Fig. 8). However, the trends of

–1.14 $\mu\text{mol L}^{-1} \text{yr}^{-1}$ in the observations as well as –1.31 resp. –1.47 $\mu\text{mol L}^{-1} \text{yr}^{-1}$ were only slightly overestimated in the model (Table 6).

Model output was used to investigate the thermal stratification and the oxygen consumption rate with a daily instead of monthly resolution. The time during which the water column at BE was stable stratified was difficult to determine, as the duration of stratification highly depended on the temperature gradient criterion assumed. Temperature gradients between 0.6 and 1.4 $^{\circ}\text{C m}^{-1}$ were tested and yielded different results (Table 7). However, duration of stratification was increasing (1 to 10.25 d decade $^{-1}$) and the onset of stratification started earlier (2.75 to 8.25 d decade $^{-1}$) for all criteria tested.

The effect of the rising temperature trend on oxygen consumption rates was relatively small. Only 13 % (0.2 $\mu\text{mol L}^{-1} \text{yr}^{-1}$) of the total oxygen decrease of –1.47 $\mu\text{mol L}^{-1} \text{yr}^{-1}$ could be attributed to an enhancement of the oxygen consumption by temperature in the model. The remaining part originated from the prescribed primary production, to which the oxygen consumption rate was tied (see Sect. 2.3).

4 Discussion

4.1 Comparisons of observations at BE with trends in the Baltic Sea

Statistical analysis of the time series at BE revealed that significant trends were present in all of the nine analysed parameters. The trends comprise physical, chemical as well as biological parameters and indicate that the whole system undergoes significant changes, resulting e.g. in altered living conditions for biota.

Temperature trends at BE were in good agreement with trends in other regions of the Baltic Sea. The positive tendency of 0.2 $^{\circ}\text{C}$ per decade lies within the range of previously reported trends (Feistel et al., 2008, ch. 9.4, p. 252ff). The same magnitudes of mean and extreme value warming tendency indicated a general shift towards warmer temperatures, which intensified in the period 1970–2010. Most of the warming in the sea surface at BE can be attributed to the spring season, as April and May were the months with the highest

temperature increase. At the same time, temperature in the bottom water did not increase as fast as at the surface, which results in an overall significant increase in the density gradient in spring. Hence, stratification starts earlier in a year, which may lead in turn to a reduced ventilation. This is discussed in context with oxygen depletion below.

5 No significant trend could be detected for salinity at BE in the median, which is in agreement with findings of the BACC author team (BACC, 2008). They report no significant changes in salinity in the 20th century at numerous monitoring stations (BACC, 2008). Salinity fluctuates in the short-term, inter-annual variability due to large-scale advection (Lehmann et al., 2013). Major saltwater inflows triggered mainly by westerly wind regimes
10 bring saline water from the North Sea further into the Baltic Sea (Lass and Matthäus, 1996). The strongest inflow occurred in January 1993, less strong events in 1965, 1969, 1973, 1976, 1980 and in 2003 (in decreasing magnitude) (BACC, 2008; Feistel et al., 2008, , ch. 10, p. 265ff). The salinity time series at BE does not show pronounced maximal salinities for these dates. It is unlikely that the major salinity inflows did not reach BE, as the time series
15 station is located at the Boknis Eck channel with a direct connection to the Belt Sea. More likely, the bottom water is not suited to track major saltwater inflows as it already reflects the characteristics of the incoming North Sea water. Apparently, an intrusion of salt water is more pronounced in the horizontal dimension than in the vertical and are hard to detect in a 1-D profile at Boknis Eck.

20 The nutrient and phytoplankton cycle, the latter indicated by the chlorophyll a concentrations at the surface, showed a typical annual seasonality. Smetacek (1984) described the annual cycle of plankton and nutrients in the Kiel Bight in several stages. The four stages previously described in Smetacek (1984) could be observed throughout the whole time span. They comprise a spring bloom, at BE indicated by high chlorophyll a concentrations
25 in March, a herbivorous copepod maximum that could not be detected by the parameters discussed here, a third stage during summer stratification, which was here identified by low nutrient concentration and comparably high chlorophyll a concentrations, as well as an autumn bloom that varied in timing, again indicated by elevated chlorophyll a concentrations. Smetacek (1984) observed constant nutrient concentrations in winter and consequently, a

similar bloom size each year during a 10 year period, which contrasted to the decreasing nutrient concentrations and decreasing chlorophyll *a* concentrations found over the longer period 1960/1986-2013.

The peak in bottom water ammonium appeared consistently with a lag of one month after increased chlorophyll *a* concentration in the surface layer and was especially strong when anoxic conditions were present. This may indicate remineralisation of organic matter after the blooms. The lag of one month after the dieback of algal blooms was in agreement with previous studies showing an increase in methane one month after an algal bloom in the bottom water found by ?, that they also attributed to remineralisation. Ammonium accumulation is known to occur during the decomposition of organic matter, when further oxidation to nitrite and nitrate is hindered by low oxygen concentrations.

Although the seasonal cycle varied only little with respect to the yearly course, the magnitude of the nutrient and chlorophyll *a* concentration did change significantly during 1980–2013 (nutrients) resp. 1960–2013 (chlorophyll *a*). In general, the concentrations of nutrients during the winter months were significantly decreasing. This decrease has been detected in several other stations of the Baltic Sea as well. For nitrate, trends in the Bornholm and Gotland basin increased until the early 1990's and decreased since then (Feistel et al., 2008, , ch. 12.2, p. 344f). Conley et al. (2002) analysed total nitrogen concentrations in the Danish waters and found a decrease from 1980 to 2003. Carstensen et al. (2006) reported a decrease of the nutrient discharges from Denmark by 50 % from 1988 to 2002. In the BE time series, nitrate measurements were only available from 1986 on, but the general decrease since then was confirmed. For phosphorous discharge, Carstensen et al. (2006) detected a decrease of 80 % which they attributed mainly to the installation of wastewater treatment plants. Further studies found phosphate to increase until the 1980s and since then showing strong fluctuations without a clear trend (Feistel et al., 2008, , ch. 12.3, p. 345). Phosphate did show stronger fluctuations than nitrate in the BE series, but the decreasing tendency was significant in the winter months.

Accompanied by this significant decrease in nutrient concentrations is a decline in chlorophyll *a* concentrations. This is most striking when comparing the means between

the two chlorophyll series 1960–1975 and 1986–2013, where the concentration fell from 5.5 ± 6.39 to $2.9 \pm 2.6 \mu\text{g L}^{-1}$. Additionally, decreasing trends for the second period were found. As lower nutrients concentrations would lead to less production and less intense algal blooms, these findings match well. HELCOM (2009) registered a decreasing trend in chlorophyll *a* concentrations since the mid 1990s for the Kattegatt and Belt Sea, with an increasing tendency from 2000 on. Wasmund and Uhlig (2003) also found a decreasing, yet nonsignificant, trend for the chlorophyll *a* concentrations in the Kattegatt and Belt Sea and attributed it to the decreasing nutrient concentrations. In general, chlorophyll *a* trends in the regions of the Danish straits are highly variable, and even opposite trends can be found for individual regions (HELCOM, 2009). Due to phytoplankton blooms lasting shorter than the sampling interval, trends in chlorophyll *a* are sensitive to the sampling date, as the peaks could have been missed. However, the general decreasing trend throughout the whole period of 56 years is still evident.

The annual cycle of Secchi depth with a minimum in March and a maximum during winter matched the findings of the chlorophyll *a* cycle. The slight decrease in Secchi depth by about 8 cm yr^{-1} in the 90 % quantile fits in magnitude with a trend published for the Swedish Baltic Sea by 8 cm yr^{-1} (Sanden and Hakansson, 1996), both indicating an increased turbidity.

The oxygen concentration declined significantly with a simultaneous increase in hypoxic and anoxic events in the bottom water during the period 1957–2013 at BE. The spreading of hypoxic and even anoxic zones in marine coastal ecosystems is known to occur worldwide and is often related to eutrophication (Diaz and Rosenberg, 2008). The Baltic Sea is affected by oxygen decline over large areas (HELCOM, 2009), which have increased since 2001. The temporal extension of hypoxia matches well with the oxygen decline at BE.

4.2 Comparison of observations at BE with BSIOM output

The BSIOM reproduced observed temperature, salinity and oxygen at the location of BE with an acceptable range of uncertainty. For temperature, it became obvious that the timing of the monthly observation is important for the magnitude of trend, and trends could differ around 30 % compared to the observed trend. The timing is especially important when

parameter variation is high, e.g. for the surface temperature. Observed temperature at the bottom showed only little variations, and trends did not depend strongly on the temporal resolution. In general, the model reproduced the measurements accurately, and can therefore be applied to look in detail in the development of temperature stratification discussed with oxygen depletion below.

Salinity was reproduced less precise than temperature (lower correlation, magnitude of trend), but as changes in the ventilation system seem to be driven by temperature changes (see below), salinity was not further considered to find reasons for the ongoing oxygen decline by model output analysis.

Oxygen trends were similar, despite the simplified oxygen parametrisation in the model. Although concentrations were overestimated, the trend in oxygen depletion is captured well by the model. However, it has to be noted that only a small fraction of the decreasing oxygen concentration trend can be attributed to a temperature enhanced oxygen consumption. Most of the oxygen depletion in the model is based on an increase in primary production. Although an increase in primary production is questionable at BE due to significantly decreasing nutrient concentrations, it cannot be excluded, as no direct measurements are available. In general, the oxygen consumption rate is captured well by the model and reflects the observed trend well, but the reasons for that cannot completely be confirmed.

4.3 Possible reasons for ongoing observed oxygen decline in the bottom water

4.3.1 Observations

First, possible processes causing oxygen depletion in the bottom water are discussed here based on the time series of observations at Boknis Eck. Processes discussed include nutrient remobilisation, the physical process of decreasing solubility of gases with increasing temperature, lower oxygen supply by altered ventilation and temperature enhanced oxygen consumption rate.

Nutrient remobilisation from the sediment due to lower oxygen concentrations in the bottom water are often cited to contribute to ongoing oxygen decline (see e.g. Conley et al.,

2002; Pitkänen et al., 2001). At BE, e.g. phosphate concentrations in the bottom water were elevated during periods of anoxia, but the general trend was significantly decreasing between 1980–2013. If remobilisation was the only process responsible for the oxygen decline, oxygen concentrations would have increased accordingly. This was not the case, thus phosphate remobilisation may not be the key process responsible for oxygen decline.

Increasing temperature also decreases the solubility of oxygen. However, the oxygen saturations showed a significant decrease as well. The oxygen saturation opposite to the oxygen concentration already takes into account changes in temperature. A decrease in the oxygen saturation means that the decrease in concentration cannot be attributed completely to the physical effect of solubility.

Rising temperatures further enhance remineralisation of organic matter that is deposited on the bottom, resulting in increased oxygen consumption (Hoppe et al., 2013). This hypothesis is further supported by the lacking trend of bottom water ammonium concentration. Despite lower nutrient input, ammonium concentrations in the bottom water did not decline, indicating that remineralisation might be enhanced by other factors and counterbalance the decrease in nutrients. Rising temperatures might be a possible explanation for this ongoing remineralisation.

Moreover, there is evidence for an alteration in the ventilation at Boknis Eck. At BE, the density gradient across the pycnocline strengthened significantly in the period 1957–2013 especially in spring, when the rise of temperature was greater at the surface than at the bottom. A stronger stratification earlier in the year hampers ventilation and therefore oxygen supply to the bottom water layer and might be a possible reason for intensified oxygen decline. A schematic overview on possible reasons for the ongoing oxygen decline despite decreasing eutrophication is given in Fig. 9.

Whether or not the variation in advection of oxygen enriched or depleted water through the Danish Straits is a possible reason for the ongoing oxygen decline at BE cannot be estimated accurately based on the one-dimensional BE data. After the main inflowing events (see Sect. 4.1), no major change could be seen in the bottom water oxygen concentrations at BE. In summary, observations indicate that the ongoing oxygen depletion might be

caused by an altered ventilation including an earlier onset of stable stratification, as well as enhanced oxygen consumption, possibly triggered by rising temperatures in the bottom water at BE.

4.3.2 Model output

- 5 The daily model output indicated a prolongation of the stratification period at BE, although the length of the stratification strongly depend on the temperature difference criteria chosen to detect the thermocline. All of the chosen criteria between 0.6 and $1.4^{\circ}\text{C m}^{-1}$ led to a prolongation and an earlier onset of stable stratification.

- The second possible reason was oxygen decline due to enhanced remineralisation rates.
- 10 In the BSIOM, oxygen consumption is only based on temperature dependent consumption rate, which is related to prescribed primary production (see Sect. 2.3). Although this parametrisation is a strong simplification and is based on the only available but sparse data set on primary production (Wasmund et al., 2011), the trends of oxygen concentration were very well captured. The reason for the increase in oxygen consumption in the model
- 15 are based on an increase in primary production, which is debatable at the location of BE. Against an increase in primary production points the fact that nutrient concentrations are significantly decreasing, when they are considered at the same time as the limiting factor (Wasmund et al., 2011). However, as direct measurements are not available at BE, it cannot be excluded that increasing primary production is the reason for the ongoing oxygen
- 20 decline. In summary, the magnitude of the oxygen consumption rate seems to be accurate in the model, but the reasons for the ongoing oxygen decline cannot be completely resolved based on the BSIOM output, as the basic assumption of increasing primary production can neither be confirmed nor rejected.

5 Conclusions

- 25 The detection of significant long-term trends in all of the studied oceanographic parameters in the period of 1957 to 2013 revealed that Boknis Eck is subjected to extensive

changes that comprise biological, biogeochemical and physical factors, with implications for the ecosystem. The observed trends for increasing temperature and decreasing oxygen concentration in the bottom water are representative for the southwestern Baltic Sea; decreasing chlorophyll *a* and nutrient concentration lay in the range of observations elsewhere, although these parameters have very variable spatial patterns in the Baltic Sea. In general, monitoring at the Time Series Station Boknis Eck is valuable to detect changes that reflect variations in large parts of the southwestern Baltic Sea.

Oxygen concentration in the bottom water at BE decreased significantly despite the decrease of nutrient concentrations. Based on the observed temporal development of the physical and biological parameters at BE, we hypothesize that enhanced remineralisation due to temperature increase and a longer lasting stratification may enhance oxygen depletion. It could be proved that the remobilisation of phosphate from anoxic sediments might act as a long term nutrient source. However, the remobilisation is unlikely to significantly enhance oxygen consumption through organic matter mineralisation by triggering phytoplankton growth, as the general trend was decreasing.

The comparison to the temporarily higher resolved model output revealed that the period of stratification had an prolonging effect, although the magnitude of the prolongation depends on the temperature criteria chosen to identify the stratification. Oxygen depletion trends were captured well by the model, but the reasons for increased oxygen consumption were only by ca. 13 % attributable to the temperature increase. The remaining part may be attributed to an increase in primary production implemented in the BSIOM. Furthermore, it could be shown that the monthly temporal resolution of BE observations may lead to inaccuracies in the trends, especially when the parameter shows high short-term fluctuations. Continuing the monthly measurements at Time Series Boknis Eck is of major importance to monitor and understand future changes in the southwestern Baltic Sea. An extension of the parameters including in situ primary production would be helpful to verify the hypothesis of increasing primary production despite decrease in nutrients as a reason for the ongoing oxygen decline.

Acknowledgements. The authors thank the captain and crew of the R/V *Littorina* and *Polarfuchs* as well as the many colleagues and numerous students who helped to continue the BE time series through various projects. We thank Christian Franzke for generously providing his MatLab scripts. The time series BE was supported by DWK Meeresforschung (1957–1975), HELCOM (1979–1995), BMBF (1995–1999), Institut für Meereskunde (1999–2003), IfM-GEOMAR (2004–2011) and GEOMAR (2012-present). BE is a LOICZ affiliated project. The Boknis Eck Time Series Station (www.bokniseck.de) is run by the Chemical Oceanography Research Unit of GEOMAR, Helmholtz-Centre for Ocean Research Kiel. We thank Viktor Smetacek and one anonymous referee for helpful comments that helped to improve the manuscript.

References

- Babenerd, B.: Increasing oxygen deficiency in Kiel Bay (Western Baltic) – a paradigm of progressing coastal eutrophication, *Meeresforschung*, 30, 121–140, 1991.
- BACC: Assessment of Climate Change for the Baltic Sea Basin, Springer, 2008.
- Bange, H. W., Hansen, H.-P., Malien, F., Lass, K., Dale, A., Karstensen, J., Petereit, C., and Friedrichs, G.: Boknis Eck Time Series Station (SW Baltic Sea): Measurements from 1957 to 2010, LOICZ-Affiliated Activities, 2011.
- Bendtsen, J. and Hansen, J. L. S.: Effects of global warming on hypoxia in the Baltic Sea–North Sea transition zone, *Ecol. Model.*, 264, 17–26, 2013.
- Bonsdorff, E., Blomqvist, E. M., Mattila, J., and Norkko, A.: Coastal eutrophication: causes, consequences and perspectives in the Archipelago areas of the Northern Baltic Sea, *Estuar. Coast. Shelf S.*, 44, 63–72, 1997.
- Bumke, K., Karger, U., Hasse, L., and Niekamp, K.: Evaporation over the Baltic Sea as an example of a semi-enclosed sea, *Contr. Atmos. Phys.*, 71, 249–261, 1998.
- Burkey, J.: Matlab Function: Seasonal Kendall Trend Test for Data with and without Serial Dependence, MatLab fileexchange, 2012.
- Carstensen, J., Conley, D. J., Andersen, J. H., and Aertebjerg, G.: Coastal eutrophication and trend reversal: a Danish case study, *Limnol. Oceanogr.*, 5, 398–408, 2006.
- Conley, D. J., Humborg, C., Rahm, L., Savchuk, O. P., and Wulff, F.: Hypoxia in the Baltic Sea and basin-scale changes in phosphorus biogeochemistry, *Env. Sci. Tech.*, 36, 5315–5320, 2002.

Ducklow, H. W., Doney, S. C., and Steinberg, D. K.: Contributions of long-term research and time-series observations to marine ecology and biogeochemistry, *Annu. Rev. Mar. Sci.*, 1, 279–302, 2009.

5 Diaz, R. and Rosenberg, R.: Spreading dead zones and consequences for marine ecosystems, *Science*, 321, 926–930, 2008.

Feistel, R., Nausch, G., and Wasmund, N.: State and Evolution of the Baltic Sea, 1952–2005: a Detailed 50-Year Survey of Meteorology and Climate, Physics, Chemistry, Biology and Marine Environment, Wiley-Blackwell (an imprint of John Wiley & Sons Ltd), 2008.

Franzke, C.: A novel method to test for significant trends in extreme values in serially dependent
10 time series, *Geophys. Res. Lett.*, 40, 1391–1395, 2013.

Garcia, H. E. and Gordon, L. I.: Oxygen solubility in seawater: better fitting equations, *Limnol. Oceanogr.*, 37, 1307–1312, 1992.

Grasshoff, K., Kremling, K., and Ehrhardt, M.: *Methods of Seawater Analysis*, Wiley-VCH, 3rd Edn., 1999.

15 Hanninen, J., Vuorinen, I., and Hjelt, P.: Climatic factors in the Atlantic control the oceanographic and ecological changes in the Baltic Sea, *Limnol. Oceanogr.*, 45, 703–710, 2000.

Hansen, H. P., Giesenhausen, H. C., and Behrends, G.: Seasonal and long-term control of bottom-water oxygen deficiency in a stratified shallow-water coastal system, *ICES J. Mar. Sci.*, 56, 65–71, 1999.

20 Hansen, J. L. S. and Bendtsen, J.: Effects of climate change on hypoxia in the North Sea – Baltic transition zone, *IOPC Ser. Earth Environ. Sci.*, 6, Copenhagen, Denmark, 2009.

HELCOM: Convention on the protection of the marine environment of the Baltic Sea area, Helsinki Convention, 1–27, 1974.

HELCOM: Eutrophication in the Baltic Sea – an integrated assessment of the effects of nutrient
25 enrichment in the Baltic Sea region, *Baltic Sea Environ. Proc.*, 115, 1–145, 2009.

Hirsch, R. M. and Slack, J. R.: A nonparametric trend test for seasonal data with serial dependence, *Water Resour. Res.*, 20, 727–732, 1984.

Hoppe, H.-G., Giesenhausen, H. C., Koppe, R., Hansen, H.-P., and Gocke, K.: Impact of change in climate and policy from 1988 to 2007 on environmental and microbial variables at the time series
30 station Boknis Eck, Baltic Sea, *Biogeosciences*, 10, 4529–4546, doi:10.5194/bg-10-4529-2013, 2013.

Jonasson, L., Hansen, J. L. S., Wan, Z., and She, J.: The impacts of physical processes on oxygen variations in the North Sea-Baltic Sea transition zone, *Ocean Sci.*, 8, 37–48, doi:10.5194/os-8-37-2012, 2012.

Karlson, K., Rosenberg, R., and Bonsdorff, E.: Temporal and spatial large-scale effects of eutrophication and oxygen deficiency on benthic fauna in Scandinavian and Baltic waters – a review, *Oceanogr. Mar. Biol. Annu. Rev.*, 40, 427–489, 2002.

Koenker, R. and Hallock, K.: Quantile regression, *Jour. Econ. Persp.*, 15, 143–156, 2001.

Krey, J.: Die Bestimmung des Chlorophyll a in Meerwasser-Schöpfproben, *Meereskundliche Arbeiten der Universität zu Kiel*, 65, 201–209, 1939.

Krey, J., Babenerd, B., and Lenz, J.: Beobachtungen zur Produktionsbiologie des Planktons in der Kieler Bucht 1957–1975, *Berichte aus dem Institut für Meereskunde*, 1, 1–20, 1980.

Kronsell, J. and Andersson, P.: Total regional runoff to the Baltic Sea, *HELCOM Indicator Fact Sheets 2011*, available at: <http://www.helcom.fi/environment2/ifs>, 2012.

Lass, H. U. and Matthäus, W.: On temporal wind variations forcing salt water inflows into the Baltic Sea, *Tellus Ser. A*, 48, 663–671, 1996.

Lehmann, A.: A three-dimensional baroclinic eddy-resolving model of the Baltic Sea, *Tellus Ser. A*, 47, 1013–1031, 1995.

Lehmann, A. and Hinrichsen, H.-H.: On the thermohaline variability of the Baltic Sea, *J. Mar. Syst.*, 25, 333–357, 2000.

Lehmann, A., Krauss, W., and Hinrichsen, H.-H.: Effects of remote and local atmospheric forcing on circulation and upwelling in the Baltic Sea, *Tellus Ser. A*, 54, 299–316, 2002.

Lehmann, A., Myrberg, K., and Getzlaff, K.: Salinity dynamics of the Baltic Sea, *Baltic Earth newsletter*, 1, 3–5, 2013.

Lehmann, A., Hinrichsen, H.-H., Getzlaff, K., and Myrberg, K.: Quantifying the heterogeneity of hypoxic and anoxic areas in the Baltic Sea by a simplified coupled hydrodynamic-oxygen consumption model approach, *J. Mar. Syst.*, 134, 20–28, 2014.

Novotny, K., Liebsch, G., Lehmann, A., and Dietrich, R.: Variability of sea surface heights in the Baltic Sea: an intercomparison of observations and model simulations, *Mar. Geod.*, 29, 113–134, 2006.

Pitkänen, H., Lehtoranta, J., and Räike, A.: Internal nutrient fluxes counteract decreases in external load: the case of the Estuarial Eastern Gulf of Finland, *Baltic Sea, Ambio*, 30, 194–301, 2001.

Rabalais, N. N., Turner, R. E., Diaz, R. J., and Justic, D.: Global change and eutrophication of coastal waters, *ICES J. Mar. Sci.*, 66, 1528–1537, 2009.

- Rheinheimer, G. and Nehring, D.: Meereskunde der Ostsee, Springer, 2nd Edn., 1995.
- Rosenberg, R.: Negative oxygen trends in Swedish coastal bottom waters, *Mar. Pollut. Bull.*, 21, 335–339, 1990.
- Rudolph, C. and Lehmann, A.: A model-measurements comparison of atmospheric forcing and surface fluxes of the Baltic Sea, *Oceanologia*, 48, 333–380, 2006.
- Sanden, P. and Hakansson, B.: Long-term trends in Secchi depth in the Baltic Sea, *Limnol. Oceanogr.*, 41, 346–351, 1996.
- Schreiber, T. and Schmitz, A.: Improved surrogate data for nonlinearity tests, *Phys. Rev. Lett.*, 77, 635–638, 1996.
- Sen, P. K.: Estimates of the regression coefficient based on Kendall's Tau, *J. Am. Stat. Assoc.*, 63, 1379–1389, 1968.
- Smetacek, V., Bodungen, B.v., Knoppers, B., Peinert, R., Pollehne, F., Stegmann, P., and Zeitzschel, B.: Seasonal stages characterizing the annual cycle of an inshore pelagic system, *Rapp. P.v. Reun. Cons. int. Explor. Mer*, 183, 126–135, 1984.
- Smetacek, V.: The annual cycle of Kiel Bight plankton: a long-term analysis, *Estuaries*, 8, 145–157, 1985.
- Tyler, J. E.: The Secchi disc, *Limnol. Oceanogr.*, 13, 1–6, 1968.
- UNESCO O.: Background Papers and Supporting Data on the International Equation of State of Sea-water 1980, UNESCO Technical Papers in Marine Science, 1981.
- Wasmund, N. and Uhlig, S.: Phytoplankton trends in the Baltic Sea, *J. Mar. Sci.*, 60, 177–186, 2003.
- Wasmund, N., Andrushaitis, A., Lysiak-Pastuszak, E., Müller-Karulis, B., Nausch, G., Neumann, T., Ojaveer, H., Olenina, I., Postel, L., and Witek, Z.: Trophic status of the south-eastern Baltic Sea: a comparison of coastal and open areas, *Estuar. Coast. Shelf S.*, 53, 849–864, 2001.
- Wasmund, N., Tuimala, J., Suikkanen, S., Vandepitte, L., and Kraberg, A.: Long-term trends in phytoplankton composition in the western and central Baltic Sea, *J. Mar. Syst.*, 87, 145–159, 2011.
- Welschmeyer, W. A.: Fluorometric analysis of chlorophyll *a* in the presence of chlorophyll *b* and pheopigments, *Limnol. Oceanogr.*, 39, 1985–1992, 1994.

Table 1. Synopsis of methods used for determining oceanographic parameters at Time Series Station Boknis Eck since 1957. n.r. = not reported, CTD = conductivity, temperature, depth, SCFA = Segmented Continuous Flow Analyser, Meth. = methanol.

Parameter	Unit	Method	Reference	Timespan
Temperature	°C	Reversing thermometer	Krey et al. (1980)	1957–1975
	°C	Electrical thermometer, CTD	HELCOM Grasshoff et al. (1999)	1979–
Oxygen	$\mu\text{mol L}^{-1}$	Winkler titration	Krey et al. (1980)	1957–
			Grasshoff et al. (1999)	
Salinity	‰	Refractometer	Krey et al. (1980)	1957–n.r.
	psu	Salinometer, CTD	Krey et al. (1980)	n.r.–
Phosphate	$\mu\text{g L}^{-1}$	Photometer ELKO Zeiss II	Grasshoff et al. (1999)	1957–7/1970
	$\mu\text{mol L}^{-1}$	SCFA	Grasshoff et al. (1999)	8/1970–
Nitrate	$\mu\text{mol L}^{-1}$	SCFA	Grasshoff et al. (1999)	1979–
Nitrite	$\mu\text{mol L}^{-1}$	SCFA	Grasshoff et al. (1999)	1979–
Ammonium	$\mu\text{mol L}^{-1}$	SCFA	Grasshoff et al. (1999)	1986–
Chlorophyll <i>a</i>	$\mu\text{g L}^{-1}$	Meth.-extraction, Photometer	Krey (1939)	1975–2009
	$\mu\text{g L}^{-1}$	Fluorometer	Welschmeyer (1994)	2009–
Secchi depth	m	Secchi disc	Tyler (1968)	1986–

Table 2. Test statistics of monthly Mann–Kendall–Tests part I. Only significant results are shown. Tau b = Kendall-coefficient for time series including ties, Sen's slope = median slope present in time series (yr^{-1}), C.I. = Confidence interval of Sen's slope.

	Tau b	p value	Sen's slope	C.I. 5%	C.I. 95%
Temperature 1 m ($^{\circ}\text{C}$)					
Jan	0.21	0.048	0.03	0	0.05
Apr	0.35	< 0.001	0.07	0.03	0.10
May	0.30	0.003	0.06	0.02	0.09
Temperature 25 m ($^{\circ}\text{C}$)					
Jan	0.23	0.026	0.03	0.00	0.06
Feb	0.20	0.044	0.03	0.00	0.06
Mar	0.22	0.016	0.03	0.01	0.06
Apr	0.31	0.001	0.04	0.02	0.06
Jun	0.23	0.026	0.03	0.00	0.05
Sep	0.25	0.005	0.04	0.01	0.06
Salinity (-)					
Mar	0.19	0.037	0.04	0.00	0.07
Apr	0.23	0.011	0.06	0.01	0.10
Oxygen concentration 25 m (μM)					
Jan	-0.27	0.011	-1.45	-2.42	-0.33
Mar	-0.29	0.002	-1.18	-1.96	-0.46
Apr	-0.31	0.001	-1.63	-2.46	-0.69
May	-0.27	0.006	-1.20	-2.35	-0.37
Jul	-0.34	< 0.001	-1.51	-2.22	-0.79
Aug	-0.20	0.030	-0.71	-1.32	-0.08
Sep	-0.35	< 0.001	-0.76	-1.31	-0.36
Oxygen saturation (%)					
Jan	-0.23	0.032	-0.26	-0.52	-0.02
Apr	-0.26	0.005	-0.33	-0.56	-0.15
May	-0.24	0.016	-0.32	-0.59	-0.06
Jul	-0.32	0.001	-0.47	-0.71	-0.23
Sep	-0.32	0.001	-0.22	-0.39	-0.10
Density gradient (kg m^{-4})					
Apr	0.32	0.001	0.002	0.001	0.003
Jul	-0.19	0.043	-0.001	-0.002	> -0.001
Oct	-0.21	0.038	-0.001	-0.003	> -0.001
Chlorophyll a I 10 m ($\mu\text{g L}^{-1}$)					
Feb	-0.50	0.016	-0.30	-0.70	-0.06
Chlorophyll a II 10 m ($\mu\text{g L}^{-1}$)					
Feb	0.30	0.021	0.06	0	0.22
Apr	-0.38	0.002	-0.11	-0.19	-0.03
May	-0.33	0.018	-0.04	-0.09	-0.01
Jul	-0.29	0.017	-0.04	-0.12	-0.01
Oct	-0.30	0.031	-0.12	-0.23	-0.01

Table 3. Test statistics of monthly Mann–Kendall–Tests part II. Only significant results are shown. Tau b = Kendall-coefficient for time series including ties, Sen's slope = median slope present in time series (yr^{-1}), C.I. = Confidence interval of Sen's slope.

	Tau b	p value	Sen' slope	C.I. 5 %	C.I. 95 %
Nitrate 10 m ($\mu\text{mol L}^{-1}$)					
Jan	−0.33	0.017	−0.17	−0.29	−0.02
Feb	−0.38	0.002	−0.26	−0.41	−0.10
Mar	−0.35	0.002	−0.18	−0.44	−0.04
Apr	−0.49	< 0.001	−0.05	−0.08	−0.03
Jun	−0.33	0.017	−0.01	−0.02	0.00
Aug	−0.31	0.008	−0.01	−0.01	0.00
Oct	−0.37	0.008	−0.01	−0.02	0.00
Nitrite 10 m ($\mu\text{mol L}^{-1}$)					
Jan	−0.29	0.050	−0.02	−0.03	0.00
Mar	−0.26	0.027	−0.02	−0.03	0.00
Apr	−0.28	0.024	0.00	0.00	0.00
Oct	−0.36	0.014	0.00	−0.01	0.00
Phosphate 10 m ($\mu\text{mol L}^{-1}$)					
Jan	−0.37	0.013	−0.02	−0.03	0.00
Mar	−0.34	0.005	−0.02	−0.04	0.00
Apr	−0.26	0.038	0.00	−0.01	0.00
Ammonium 10 m ($\mu\text{mol L}^{-1}$)					
Jan	−0.31	0.035	−0.09	−0.16	−0.01
Feb	−0.49	0.000	−0.12	−0.18	−0.07
Mar	−0.37	0.002	−0.02	−0.03	0.00
Apr	−0.38	0.002	−0.01	−0.03	0.00
Aug	0.25	0.039	0.00	0.00	0.01
Phosphate 25 m ($\mu\text{mol L}^{-1}$)					
Jan	−0.27	0.074	−0.01	−0.03	0.00
Feb	−0.44	0.000	−0.02	−0.03	−0.01
Mar	−0.42	0.000	−0.03	−0.05	−0.01
Apr	−0.25	0.042	−0.01	−0.03	0.00
Jun	0.29	0.034	0.02	0.00	0.04
Sep	−0.25	0.030	−0.12	−0.25	−0.01

Table 4. Descriptive and test statistics for Mann–Kendall–Test (MKT) and quantile regression. Std. = Standard deviation, filled = Time series after gap filling described in Sect. 2.2, Tau b = Kendall-coefficient for time series including ties, Sen's slope = median slope present in time series (yr^{-1}), p.t. = pooled trends with bootstrapping of 500 generated time series described in Sect. 2.2. * denotes significance on the 0.1 level for quantile regression.

	Temperature °C	Temperature °C	Salinity psu	Oxygen μM	Chlorophyll <i>a</i> I $\mu\text{g L}^{-1}$	Chlorophyll <i>a</i> II $\mu\text{g L}^{-1}$
Depth	1 m	25 m	25 m	25 m	10 m	10 m
Start date	30 Apr 1957	30 Apr 1957	30 Apr 1957	30 Apr 1957	31 Mar 1960	19 Apr 1988
End date	6 Feb 2013	6 Feb 2013	6 Feb 2013	6 Feb 2013	2 Dec 1975	26 Jun 2012
Mean	9.74	7.02	21.55	183.52	5.47	2.86
Std.	6.00	3.64	2.35	116.95	6.39	2.06
Missing values [%]	17.91	18.69	19.22	19.35	5.05	15.28
Mean filled	9.57	7.00	21.53	186.59	5.46	2.68
Std. filled	5.90	3.37	2.17	112.77	6.31	2.10
MKT						
homogeneity	no	yes	yes	no	yes	no
Tau b seasonal	0.15	0.19	0.01	−0.22	0.11	−0.16
p value	< 0.001	0.273	0.943	0.238	0.408	0.470
Sen's slope	0.02	0.02	0.002	−0.91	0.07	−0.04
Quantile regression						
90 % quantile data	0.002	n.d.	−0.001	−0.052	−0.011*	−0.007*
p.t. 95 %	0.003	n.d.	0.002	0.064	0.008	0.004
p.t. 5 %	−0.003	n.d.	−0.002	−0.063	−0.008	−0.004
10 % quantile data	0.001	n.d.	0.002*	−0.066*	−0.001	−0.002
p.t. 95 %	0.003	n.d.	0.002	0.051	0.043	0.016
p.t. 5 %	−0.003	n.d.	−0.002	−0.052	−0.040	−0.018

Table 5. Descriptive and test statistics for seasonal Mann–Kendall–Test (MKT) and linear regression of winter (December, January, February, DJF mean) concentrations. Percentage of missing values in brackets refer to the part of the time series used for statistic analysis. Std. = standard deviation, DJF = December, January, February.

	Phosphate μM	Phosphate μM	Nitrate μM	Nitrite μM	Ammonium μM	Ammonium μM
Depth	10 m	25 m	10 m	10 m	10 m	25 m
Start date	30 Apr 1957	30 Apr 1957	12 Mar 1979	7 Jan 1986	12 Mar 1979	12 Mar 1979
End date	6 Feb 2013	6 Feb 2013	6 Feb 2013	6 Feb 2013	6 Feb 2013	6 Feb 2013
Mean	0.39	1.85	2.10	0.20	0.80	4.84
Std.	0.42	3.40	3.43	0.27	1.48	5.15
Missing values [%]	32.8 (7.5)	34.3	48.1 (18.6)	7.7	9.7	11.0
Mean filled	0.46	1.55	2.13	0.21	0.95	4.97
Std. filled	0.45	1.72	3.20	0.27	1.43	5.10
Lineare Regression (DJF)						
slope yr^{-1}	−0.24	−0.22	−1.54	−0.07	−1.12	−0.73
Pearson's R	−0.72	−0.61	−0.54	−0.37	−0.59	−0.32

Table 6. Comparison of linear trends in observed and modelled parameters temperature (surface and bottom layer), salinity and oxygen concentration (bottom layer). To ensure comparability, trends only relate to the period 1970–2010, limited by the model output. Note that the bottom layer is at a depth of 25 m in the observations but 21–24 m in the model. O = Observations, M = BSIOM output, M./O. = Model output only on days with BE observations.

	Temperature surface °C	Temperature bottom °C	Salinity bottom –	Oxygen bottom μmol L ^{−1}
Trend O. yr ^{−1}	+0.07	+0.03	+0.04	−1.14
Trend M. yr ^{−1}	+0.04	+0.03	−0.04	−1.32
Trend M./O. yr ^{−1}	+0.06	+0.03	−0.03	−1.47
Mean±Std. O.	9.87 ± 6.0	7.14 ± 3.4	21.57 ± 2.3	74.15 ± 117.0
Mean±Std. M.	9.97 ± 6.3	5.91 ± 2.5	22.04 ± 2.7	252.34 ± 79.8

Table 7. Trends (1970–2010) and length of stratification period in the BSIOM output depending on different temperature criteria used to detect stable stratification. temp. = temperature, strat. = stratification, doy = day of year, d = days., dec. = decade.

Temp. criterion $^{\circ}\text{C m}^{-1}$	Begin strat. doy	End strat. doy	Mean duration d	Trend onset strat. d dec.^{-1}	Trend end strat. d dec.^{-1}	Trend duration d dec.^{-1}
0.6	97.9	316.6	216	−6.0	2.0	8.0
0.8	108.1	309.1	201	−8.3	2.0	10.3
1.0	121.1	301.9	181	−2.8	−0.8	1.8
1.2	129.6	296.1	166	−3.0	−1.0	2.0
1.4	136.1	293.3	157	−3.8	0.3	4.3

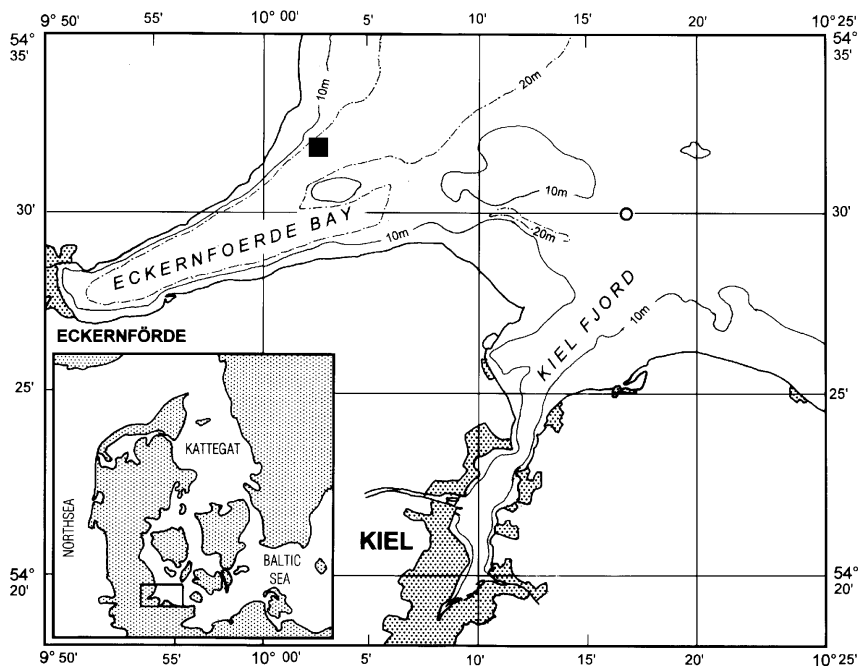


Figure 1. Location of the Boknis Eck Time Series Station at the entrance of Eckernförde Bay in the southwestern Baltic Sea, indicated by black square. (from: Hansen et al., 1999)

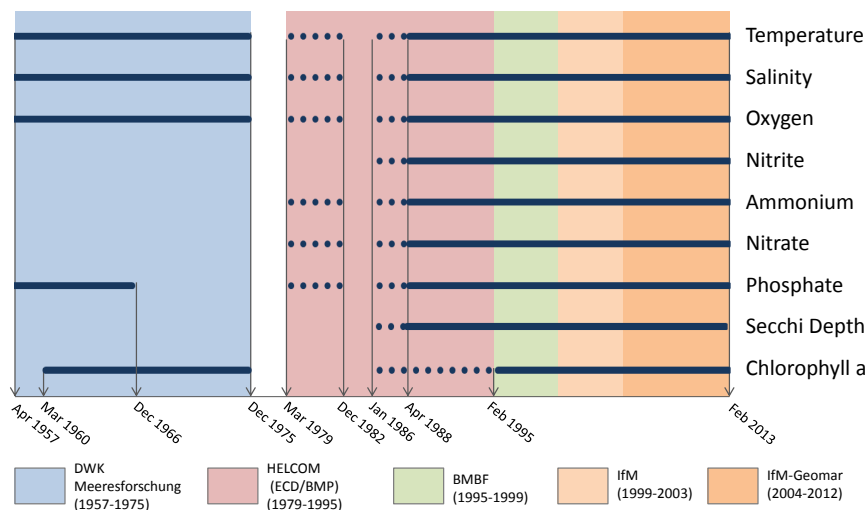


Figure 2. Synopsis of physical, chemical and biological time series at Boknis Eck. Solid lines indicate regular monthly measurements with only up to two following months missing (rare), dotted lines indicate only very irregular measurements with large gaps. Colors represent financial support by different funders. DWK = Deutsche Wissenschaftliche Kommission, HELCOM = Helsinki Commission, BMBF = Bundesministerium für Bildung und Forschung, IfM = Institut für Meereswissenschaften.

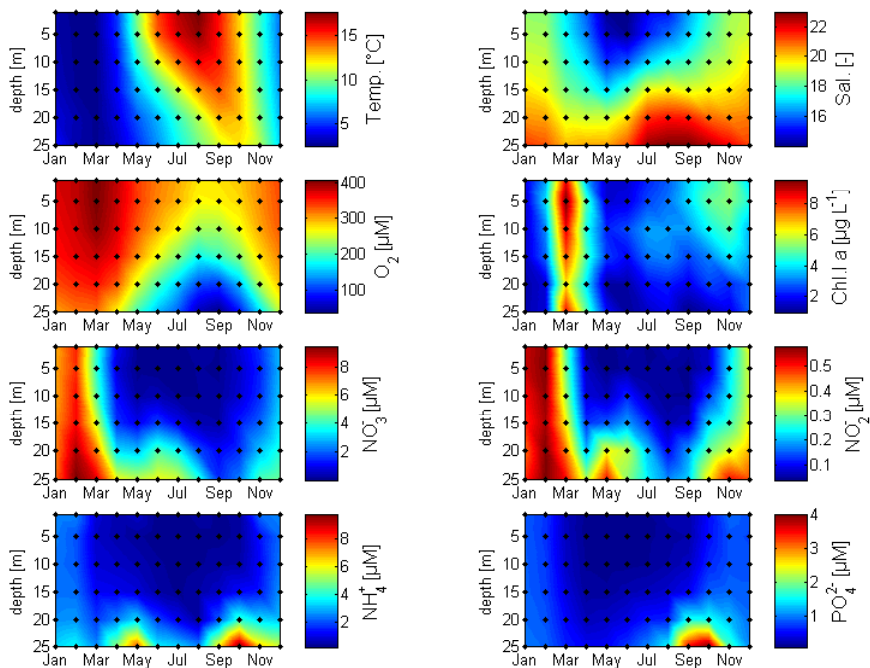


Figure 3. Mean seasonal cycle of temperature (1957–2013), salinity (1957–2013), oxygen (1957–2013), chlorophyll *a* (1960–2013), nitrate (1979–2013), nitrite (1986–2013), ammonium (1979–2013) and phosphate (1957–2013).

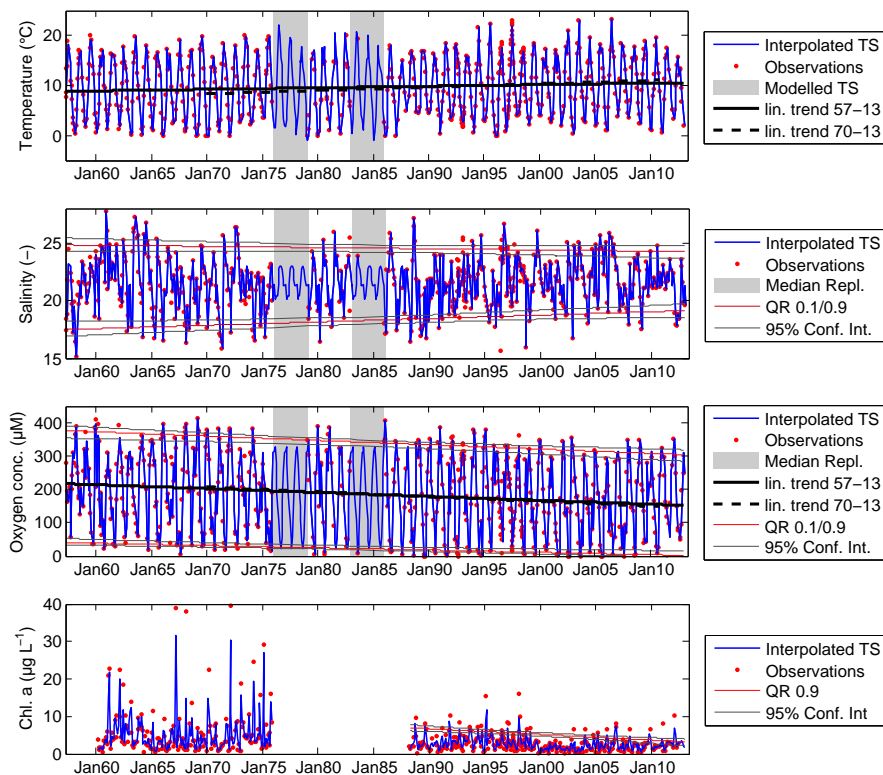


Figure 4. Time series of temperature (1 m), salinity (25 m), oxygen (25 m) and chlorophyll *a* concentration (10 m). Shown are various statistical results discussed in Sect. 3, e.g. quantile regression (QR) or linear trends over different time spans. TS = Time Series, Median Repl. = Median Replacement, Conf. Int. = Confidence Interval of quantile regression, Chl. *a* = Chlorophyll *a*.

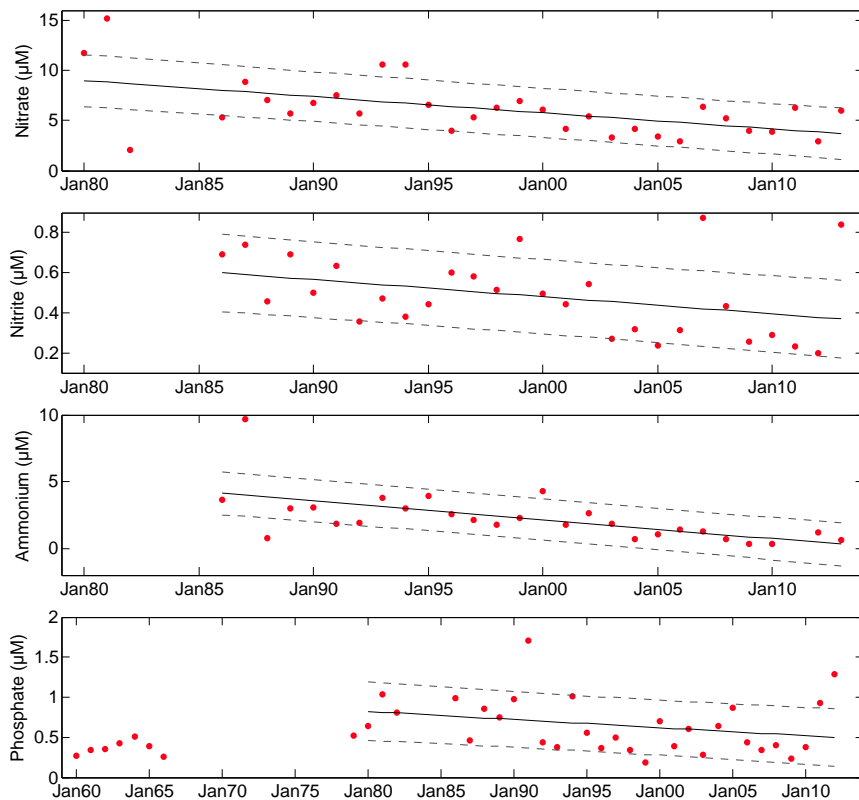


Figure 5. Average winter concentration (December, January, February, DJF, red dots) of nutrients at time series station Boknis Eck, as well as linear decreasing trends (— linear trend, — — 95% confidence interval). Note different x-axis for phosphate.

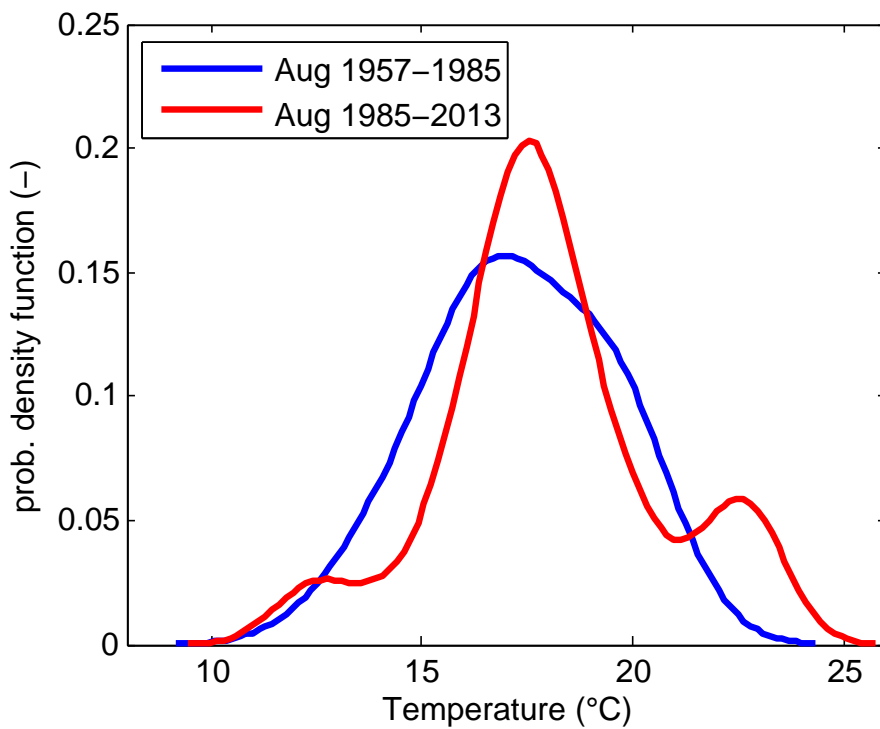


Figure 6. Normalised temperature distribution for observations at BE in August for the first half (blue) and the second half (red) of the time series at the surface water (1 m).

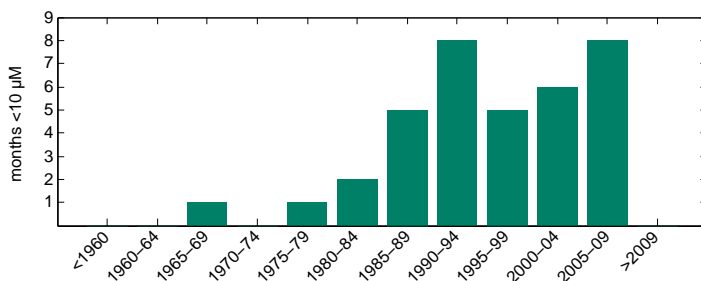


Figure 7. Increasing number of months with oxygen concentrations in 25 m depth below 10 µmol L⁻¹ at BE in 5 year periods. Note that in the periods 1970–1974 and 1980–1984, measurements were not continuously available.

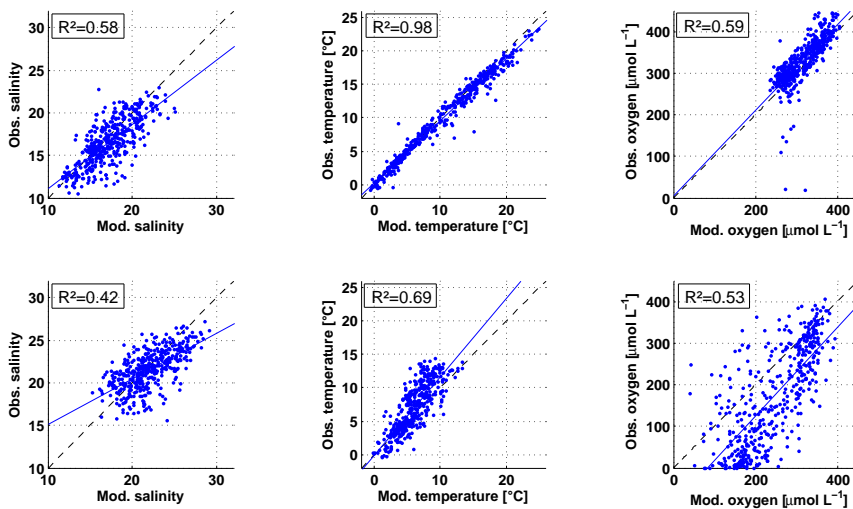


Figure 8. Linear regression of model output (BSIOM at location of BE) vs. observations (BE time series) for salinity, temperature and oxygen concentration. The first row shows surface, the second one bottom layer comparison. Note that in the model, the bottom layer is 21–24 m while it is 25 m in the observations. Obs. = Observation, Mod. = Model output.

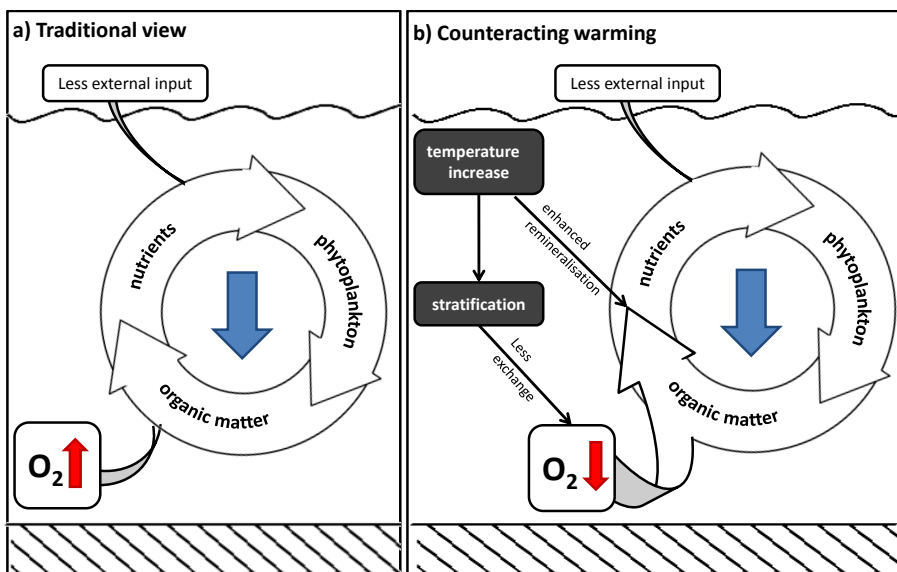


Figure 9. Schematic overview of possible causes for ongoing oxygen decline: **(a)** the traditional view of declining eutrophication: decreasing nutrient input, less phytoplankton and less organic matter leading to less oxygen consumption and thus rising oxygen concentration. **(b)** Alteration by warming temperature (dark grey): Rising temperature on the one hand enhances remineralisation, thus increases oxygen consumption, on the other hand increases stratification stability and hampers oxygen supply from surface waters.